PERGAMON

Planetary and Space Science 47 (1999) 1377–1387

Planetary and Space Science

Galileo plasma wave observations of iogenic hydrogen

T. Chust[a,*], A. Roux[a], S. Perraut[a], P. Louarn[b], W.S. Kurth[c], D.A. Gurnett[c]

[a]*Centre d'étude des Environnements Terrestre et Planétaires, CNRS et UVSQ, 10–12 Avenue de l'Europe, F-78140, Vélizy, France*
[b]*Centre d'Etude Spatiale des Rayonnements, CNRS, 9 Avenue du Colonel Roche, F-31028, Toulouse, Cedex 4, France*
[c]*Department of Physics and Astronomy, University of Iowa, Iowa City, IA 52242, USA*

Received 1 September 1998; received in revised form 1 March 1999; accepted 19 March 1999

Abstract

The Galileo plasma wave instrument has detected intense electromagnetic wave emissions approximately centered on the second and fourth harmonics of the local proton gyrofrequency during the close equatorial flyby of Io on 7 December 1995. Their frequencies suggest these emissions are likely generated locally by an instability driven by non thermal protons. Given that this process occurs close to Io, we suggest that hydrogen-bearing compounds, escaping from Io, are broken up/ionized near this moon, thereby releasing protons. Newly-created protons are thus injected in the Jovian corotating plasma with the corotation velocity, leading to the formation of a ring in velocity space. Several electromagnetic wave–particle instabilities can be driven by a ring of newborn protons. Given that the corotating plasma is sub-Alfvénic relative to Io, the magnetosonic mode cannot be destabilized by this proton ring. The full dispersion relation is studied using the WHAMP program (Rönmark, 1982. Rep. 179. Kiruna Geophys. Inst., Kiruna, Sweden) as well as a new algorithm that allows us to fit the distribution function of newborn protons in a more realistic way. This improvement in the ring model is necessary to explain the relative narrowness of the observed spectral peaks. The measured E/B ratio is also used to identify the relevant instability and wave mode: this mode results from the coupling between the ion Bernstein and the ion cyclotron mode (IBCW). To our knowledge this mode has not yet been studied. From the instability threshold an estimate of the density of newborn protons around Io is thus given; at about 2 Io radii from the surface and 40°W longitude from the sub-Jupiter meridian, this density is found to be $\geq$0.5% of the local plasma density ($\sim$4000 cm^{-3}), namely $\geq$20 cm^{-3}. Assuming a stationary pickup process and a r^{-n} distribution of pickup protons within several Io radii of Io's wake, this implies that more than 10^{26} protons/s are created around Io. The ultimate origin of these protons is an open issue.

1. Introduction

Jupiter's innermost Galilean moon, Io, is well known for the active volcanoes, the lakes of molten sulfur and the vast fields of sulfur dioxide snow covering its surface. Io is believed to be the major source of the heavy ions (sulfur and oxygen ions, mainly) in the Jovian magnetosphere. Although the existence of a tenuous SO_2 neutral atmosphere around Io is well established, the existence of H_2S (a common volcanic gas along with SO_2) in the composition of Io's atmosphere still remains a controversial issue (see Lellouch, 1996 and references therein). The detection of H_2S in solid phase, from measurements at 3.9 μm, has been claimed by Nash and Howell (1989) and Salama et al. (1990), even though the temperature and pressure conditions of the surface material of Io are above the sublimation point of pure H_2S. On the other hand, no gaseous H_2S has been detected by millimeter-wave observations (Lellouch et al., 1992). This disagreement about the existence of H_2S and hydrogen is at the origin of the present paper. Recent observations based upon a new focal instrument implemented on the Hubble Space Telescope have given evidence of glowing hydrogen gas at the Io poles (Roesler et al., 1999). Here, we use the Galileo Plasma Wave Subsystem (PWS) to investigate the plasma wave emissions in the low frequency range. More details about the PWS experiment can be found in Gurnett et al. (1992). During

* Corresponding author.
E-mail address: tch@cetp.ipsl.fr (T. Chust)

0032-0633/99/$20.00
PII: S0032-0633(99)00059-8

the closest approach of Io on 7 December 1995, the PWS experiment made a detailed survey of plasma wave emissions at frequencies above 5 Hz. Taking advantage of the possibility of measuring the electric and magnetic components, we estimate the E/B ratio and use it to identify the nature of the emitted waves and their relation to the pickup process of iogenic hydrogen.

2. Galileo plasma wave observations

The Galileo orbiter flew by Io at a minimum distance of about 900 km during its first inbound pass through the Io torus. Its trajectory was not far from radial towards Jupiter and passed Io downstream in the equatorial region. As originally suggested by the Pioneer 10 radio science measurements (Kliore et al., 1975), the plasma environment of Io presents a strong upstream/downstream asymmetry: a cold, near-stagnant and dense plasma structure ($n > 4 \times 10^4$ cm^{-3}) extends far away from Io in the wake direction (see Gurnett et al., 1996; Frank et al., 1996; Louarn et al., 1997; Hinson et al., 1998), whereas no extended dense region is found upstream (Louarn et al., 1997; Hinson et al., 1998). Fig. 1 shows the calibrated/filtered dynamic power spectra of the waves as Galileo flew by Io. The frequency range displayed is from 5 to 200 Hz. The top panel shows the data from the magnetic antenna, whereas the bottom panel shows the data from the electric one. The wave spectrum analyzer toggles between the electric and magnetic antennas every 18.666 s. In order to help visualize the highest frequency signals, the calibrated spectra have been multiplied by the function $(2f/75+1/3)^2$, which compensates for the average slope (of the calibrated power spectra) and reduces the relatively strong low-frequency noise ($f \leq 10$ Hz). It has to be stressed that these spectra are obtained via several filters having different frequency resolutions, depending on their central frequencies. The vertical width of the rectangular color patterns displayed in Fig. 1 are proportional to the frequency resolution. The line at about 130 Hz on the magnetic data is due to a spurious noise. Although there is a large level of spurious instrumental noise, tending to hide the natural emission, this figure gives a good overview of the events we are dealing with. The entry into, and the exit from, the geometrical wake are

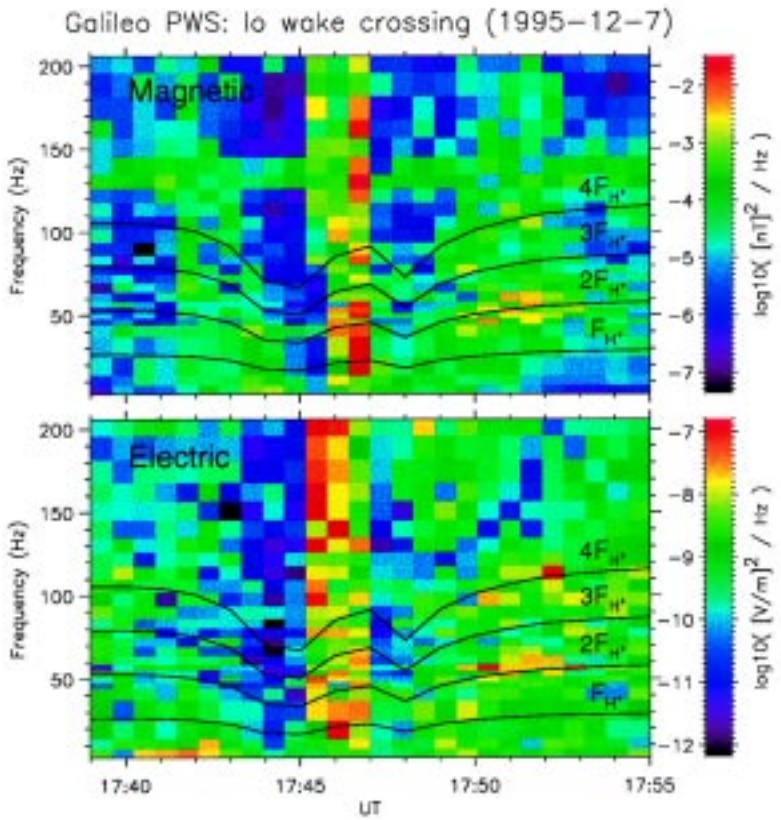

Fig. 1. Calibrated/filtered dynamic power spectra of the waves as Galileo flew through the Io wake. The top (bottom) panel shows the data from the magnetic (electric) antenna. The entry into, and the exit from the geometrical wake are at 17:44:22 and 17:48:31 UT, respectively. The superimposed curves indicate the first four harmonics of the local proton gyrofrequency.

at 17:44:22 and 17:48:31 UT, respectively. The closest approach to the moon is at 17:45:46 UT and the wake axis closest approach is at 17:46:31 UT. The first four harmonics of the local proton gyrofrequency measured from the Galileo magnetometer (Kivelson et al., 1992) are plotted as dark lines. The variations of these lines correspond to the perturbation of the Jovian magnetic field due to Io (Kivelson et al., 1996a). It is, however, difficult to ascertain whether Io has an intrinsic magnetic field because the plasma flow disturbs the magnetic field (Frank et al., 1996; Kivelson et al., 1996b). The intense burst of broadband electromagnetic wave emissions, from about 17:45:30 to 17:47:30 UT, is associated with intensive magnetic field-aligned bidirectional energetic (>15 keV) electron beams (Williams et al., 1996; Gurnett et al., 1996). The origin of these beams observed in the middle of the wake and their relation to waves is beyond the scope of this paper. We will only focus on the intense electromagnetic wave emissions that are approximately visible at two and four times the local proton gyrofrequency ($F_{H^+} \sim 25$ to 29 Hz), from about 17:50:00 to 17:54:00 UT, as Galileo was leaving the stagnation region of the Jovian corotating plasma (i.e. just after the exist from the cold plasma wake). Before the entry into the wake, no such emission is detected from the spectrum analyzer. The power spectral peak observed at about $2F_{H^+}$ is approximately 10 times more intense than that observed at about $4F_{H^+}$. For both emissions, the ratio of the electric to the magnetic field component E/B has the same order-of-magnitude, typically 2 to 8×10^6 m/s. The maximum intensities for the magnetic and electric field components are about 2×10^{-3} nT^2/Hz and 6×10^{-8} (V/m)^2/Hz, respectively.

In addition to the filter banks used to build Fig. 1, wave form data were registered during selected time periods, in particular during flybys. During the Io flyby, a snapshot of 0.274 s of wave form data was registered every 4/3 s at a rate of 3.15 kHz. Fig. 2 shows some examples of wave form data which have been Fourier transformed for the sake of comparison with data from the filter banks. Spectra from wave form data have a better frequency resolution and, as indicated above, they are collected every 4/3 s instead of 18.666 s, for the filter banks. Because of telemetry shortage, however, wave form data are digitized with a small numbers of bits (4) and are not calibrated. Thus, information on wave amplitude only comes from filter bank data. Thanks to their better time resolution the Fourier transformed wave form data show evidence of a very irregular electromagnetic wave activity at frequencies above F_{H^+}. Before the wake crossing the frequency is highly variable, as evidenced in panels a and b of Fig. 2. After the wake crossing the observed frequencies are more stable, consistent with data from the spectrum analyzer. For the time interval where the

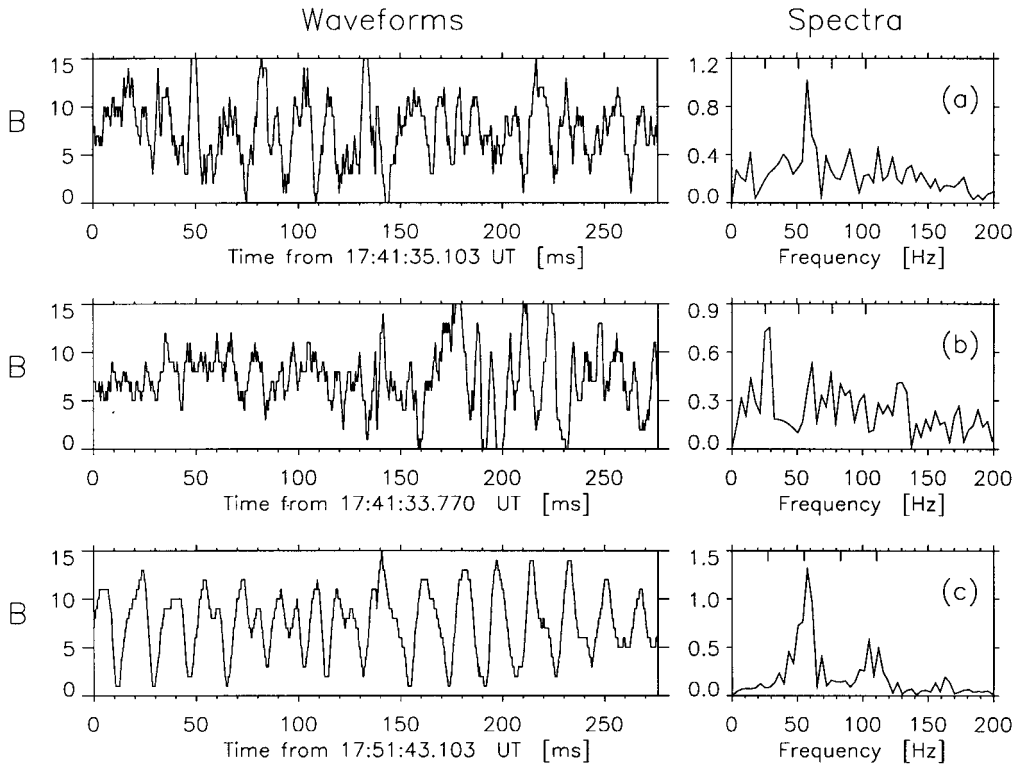

Fig. 2. Wave form data (left panels) and corresponding wave spectra (right panel). The mean values of the waveforms have been removed before performing the Fourier transforms. The ticks at the top of the right panels indicate the first four harmonics of the local proton gyrofrequency.

calibrated data show the intense spectral peaks after Io flyby, at about $2F_{H^+}$ and $4F_{H^+}$, the two data sets (filter bank data and Fourier transformed wave form data) give the same result; spectral peaks are well visible at about $2F_{H^+}$ and $4F_{H^+}$ (panel c).

In conclusion, during the close flyby of Io on 7 December 1995, the Galileo plasma wave instrument detected, outside the Io wake, electromagnetic wave activity at frequencies related to F_{H^+}. In particular, from about 17:50:00 to 17:54:00 UT, i.e. after the wake crossing at about 2 Io radii ($R_{Io} \simeq 1800$ km) from Io's surface, intense electromagnetic wave emissions approximately centered at $2F_{H^+}$ and $4F_{H^+}$ have been clearly identified. Owing to their frequencies, these emissions are likely to be generated locally by an instability driven by non thermal protons. Given that this process occurs close to Io, we suggest that hydrogen-bearing compounds, escaping from Io, are broken up/ionized near this moon, thereby releasing protons. Newly-created protons are thus injected in the Jovian corotating plasma with the corotation velocity, leading to the formation of a ring in velocity space. We will show that this type of assumed distribution accounts for the properties of the observed waves.

3. Wave instabilities for ring protons

Several electromagnetic wave–particle instabilities can be driven by a ring of newborn protons. The present paper is an attempt to identify the specific instability responsible for the observations presented above.

3.1. Preliminaries

Since the corotating plasma in the vicinity of the orbit of Io is moving approximately in a direction perpendicular to the magnetic field ($\mathbf{B}_0$), the distribution function of newborn ions, initially at rest with respect to Io, is ring-shaped around the magnetic field, with only a small parallel drift velocity that will be neglected hereafter for the sake of simplicity. The ring velocity (V_{ring}) is thus approximately equal to the corotation velocity with respect to Io ($|\mathbf{V}_c|$). In general, this is a very unstable configuration and ion cyclotron waves are expected to grow and to scatter the particles, in pitch angle and in energy, which reduces the wave growth. In a plasma containing several components, such as the Jovian corotating plasma near Io, we do not expect to get a positive growth rate near every gyrofrequency of the newly-picked up ions but only near the gyrofrequencies of the heavier and denser ones. Indeed, at low frequencies (< 5 Hz) strong ion cyclotron waves were observed close to $F_{SO_2^+}$ and F_{SO^+} by the Galileo magnetometer over a region extending up to more than 15 R_{Io} from Io (Kivelson et al., 1996b). The fact that ion cyclotron waves (ICWs) are possibly destabilized by pickup protons is, therefore, unexpected. Furthermore, proton ICWs are not expected to grow at frequencies above F_{H^+}.

Ion cyclotron harmonic wave generation by ring protons in space plasmas has been considered by Perraut et al. (1982), McClements and Dendy (1993) and McClements et al. (1994), referring to the magnetoacoustic cyclotron instability intensively studied in fusion plasmas (see Dendy et al., 1994 and references therein). Unfortunately, this mechanism where perpendicular propagating fast Alfvén waves are in resonance with ion Bernstein waves at cyclotron harmonics of the ring ions requires a ring velocity (V_{ring}) much larger than the Alfvén speed (V_A), which is far from being the case here (see Table 1).

Thus, a quick analysis based upon the well-known instabilities does not provide an obvious explanation of the observations. We investigate, therefore, the full dispersion relation.

3.2. Study of the dispersion relation using WHAMP

In a first step, the dispersion relation corresponding to the interaction between the Jovian plasma flowing around Io and the newborn ions has been computed with the WHAMP program (Rönmark, 1982). This program solves the full dispersion relation in a multicomponent magnetized plasma described by the Vlasov kinetic theory. The Jovian equilibrium plasma considered here has been assumed to be Maxwellian with temperatures of 100 eV for the ions and 10 eV for the electrons (Bagenal, 1994; Thomas, 1995; Frank et al., 1996). This corotating plasma contains about 10% of H^+, the dominant ions being oxygen and sulfur ions (Bagenal, 1995; Frank et al., 1996). Since we are concerned with 'high frequency' waves ($\geq F_{H^+}$), only one heavy ion species has been taken into account (O^+) in the calculations. This assumption stems from

Table 1
Summary of the most important physical parameters used for modelling the background torus plasma near Io

B_0 (nT)	n_e (cm^{-3})	n_{H^+} (%)	n_{O^+} (%)	T_e (eV)	T_{H^+} (eV)	T_{O^+} (eV)	V_c[a] (km/s)	V_A (km/s)
1700	4000	10	$90-\varepsilon_{H^+}^{ring}$	10	100	100	57	~ 150

[a] The corotation velocity is given with respect to Io.

the fact that the contributions of the heavy ions (picked up and corotating) are roughly indiscernible for the wave–particle interactions at work in the frequency range of interest (above F_{H^+}). For the values of the magnetic field intensity (B_0) and the electron plasma density (n_e), we have taken 1700 nT (Kivelson et al., 1996a) and 4000 cm^{-3} (Frank et al., 1996), respectively, which corresponds to representative values observed just outside the Io wake. Thus, for the background torus plasma considered here, $V_A \sim 150$ km/s. All these parameters used in the calculations for modelling the background torus plasma near Io are summarized in Table 1.

The assumed fraction of pickup protons ($\varepsilon_{H^+}^{ring}$) is distributed in the perpendicular direction on a ring with the local corotation velocity ($V_{ring} = |\mathbf{V}_c| \sim 57$ km/s), which approximately corresponds to a ring energy ($E_{ring} = \frac{1}{2}MV_{ring}^2$) of 17 eV. The ring model used by the WHAMP program being defined by the difference of two Maxwellian functions, its perpendicular velocity dispersion is comparable to the ring velocity itself. Thus, this model does not allow the description of narrow ring-shaped distribution functions. The ring distribution function used is displayed in Fig. 3. Let us define the perpendicular temperature of the ring ($T_\perp^{ring}$) as the average value of $\frac{1}{2}M(v_\perp - V_{ring})^2$. Therefore, one gets for this distribution function $T_\perp^{ring} \simeq E_{ring}/3$. The parallel temperature of the ring ($T_\parallel^{ring}$) is a free parameter that parametrizes the anisotropy. We assume all along that the threshold value for a substantial instability is a growth rate $\gamma \geq 10^{-3}\Omega_{H^+}$; this hypothesis will be justified afterwards.

The dispersion relation obtained in this way shows that ICWs could be excited at $\sim F_{H^+}$ for $\varepsilon_{H^+}^{ring} = 1\%$ when $T_\parallel^{ring} \leq 0.08$ eV. In fact, for $T_\parallel^{ring} < 0.08$ eV (strong anisotropy) the dispersion relation displays other solutions, connected to electrostatic ion Bernstein waves (they are electrostatic, excited near the harmonics of F_{H^+} and propagate obliquely relative to $\mathbf{B}_0$ with strong finite Larmor radius effects, i.e. their perpendicular wave number is such as $k_\perp V_{ring} \geq \Omega_{H^+} = 2\pi F_{H^+}$), that have a much greater growth rate than the proton ICWs. Fast diffusion is thus expected, which will flatten the ring and increase $T_\parallel^{ring}$ to a few eV, thereby quenching these initially growing waves. The stable existence of such electrostatic waves around Io is indeed unlikely because: (1) they should be excited around every harmonic of F_{H^+} and furthermore, their observation would be strongly affected by Doppler-shifts ($\Delta F/F_{H^+} \geq 1$); our observation could only account for the first harmonic; (2) the observed E/B ratio is smaller than 10^7 m/s, which does not correspond to these electrostatic waves excited by a strong anisotropy of ring protons ($E/B \geq 10^8$ m/s). In what follows we will thus take $T_\parallel^{ring} = 2$ eV, as a standard value; for this value the above quoted electrostatic instability is quenched. It has to be stressed that this conclusion on $T_\parallel^{ring}$ is valid independently of the precise form of the pickup distribution function we have considered. The electrostatic waves which initially diffuse the freshly-picked up protons are mainly determined by the anisotropy of ring protons.

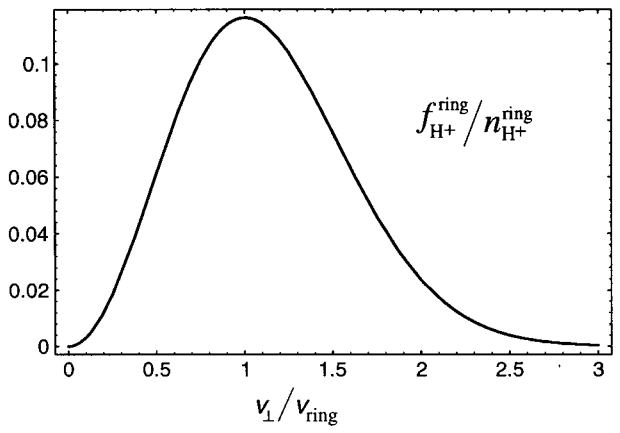

Fig. 3. Normalized ring distribution function we have used in the WHAMP computations for the pickup protons.

This preliminary analysis of the dispersion relation has led us to investigate the transient regime when the newborn protons freshly-picked up by the Jovian background corotating plasma can produce, over a short time, a very anisotropic ring. We have seen that electrostatic (like-ion Bernstein) waves rapidly heat the parallel distribution, so one asks now what waves are unstable once $T_\parallel^{ring} = 2$ eV. Indeed, as the anisotropy becomes finite ($T_\parallel^{ring} = 2$ eV > 0.08 eV) due to rapid pitch angle diffusion, unstable ICWs are no more found for realistic densities of pickup protons ($\varepsilon_{H^+}^{ring} < 33\%$). Nevertheless, for intermediate values of the density ($\varepsilon_{H^+}^{ring} \geq 2.2\%$), another branch of the dispersion relation is found to be destabilized. It corresponds to quasi-electrostatic waves having a small torsional magnetic field component ($E/B \sim 5 \times 10^6$ m/s) that grow at F_{H^+}. These waves propagate in a nearly perpendicular direction (also with strong finite Larmor radius effects) and are only weakly affected by changing significantly the anisotropy value. These waves are also found at the second harmonic of F_{H^+} but, at this frequency, they are damped. They are probably ion Bernstein waves coupled with the ion cyclotron waves associated with the ring protons (IBCWs). To our knowledge these waves have not yet been studied. In Fig. 5, the corresponding dispersion relation is presented for $\varepsilon_{H^+}^{ring} = 2.5\%$. It has to be stressed that the ICW and this IBCW are modes for which wave–proton gyroresonant interactions should play an important role. A realistic ring model is thus of crucial importance for defining their propagative properties,

in particular, for defining their growth rate. Transient electrostatic waves due to initially strong anisotropy are expected to diffuse rapidly the freshly-picked up protons. The form of a realistic pickup distribution function has to be thought of as resulting from this transient regime. The proton ring distribution function used in WHAMP's computations (Fig. 3) has intrinsically (1) a large perpendicular spread ($\sim V_{\mathrm{ring}}$) and (2) a relatively asymmetric shape with respect to the injection velocity (V_{ring}) so that there are slightly more particles for $v_\perp > V_{\mathrm{ring}}$ than for $v_\perp < V_{\mathrm{ring}}$. In fact, energy diffusion of freshly-picked up particles is usually slower than pitch angle diffusion and very likely towards smaller energies. The ring-shaped distribution function of the pickup protons is thus expected (1) to be relatively narrow in the perpendicular direction ($T_\perp^{\mathrm{ring}} < T_\parallel^{\mathrm{ring}} \ll E_{\mathrm{ring}} \sim 17$ eV) and (2) to have more particles at positive density gradient ($v_\perp < V_{\mathrm{ring}}$) than at negative density gradient ($v_\perp > V_{\mathrm{ring}}$). Therefore, using the ring model compatible with WHAMP, the threshold values determined on the pickup proton density for unstable IBCWs and ICWs (2.2 and 33%, respectively) are certainly not very accurate.

3.3. More realistic ring model

In view of the lack of flexibility of WHAMP in fitting the distribution function of the newborn ions, we have built a new algorithm to solve the same full dispersion relation but using for the pickup protons the distribution function given by:

$$f_{\mathrm{H}^+}^{\mathrm{ring}}(v_\parallel, v_\perp) = \frac{n_e \epsilon_{\mathrm{H}^+}^{\mathrm{ring}} \alpha_\perp^{-1}}{\pi^{3/2} \Delta v_\parallel \Delta v_\perp^2} \times \exp\left(\frac{-v_\parallel^2}{\Delta v_\parallel^2}\right)$$

$$\times \exp\left(\frac{-(v_\perp - V_{\mathrm{ring}})^2}{\Delta v_\perp^2 [1 + (d_\perp - 1) Y(v_\perp - V_{\mathrm{ring}})]^2}\right), \quad (1a)$$

where

$$\alpha_\perp = \exp\left(\frac{-V_{\mathrm{ring}}^2}{\Delta v_\perp^2}\right) + \sqrt{\pi}\frac{V_{\mathrm{ring}}}{\Delta v_\perp}\mathrm{erfc}\left(\frac{-V_{\mathrm{ring}}}{\Delta v_\perp}\right)$$

$$+ (d_\perp - 1)\left(d_\perp + 1 + \sqrt{\pi}\frac{V_{\mathrm{ring}}}{\Delta v_\perp}\right) \quad (1b)$$

is a normalisation factor, $\Delta v_\parallel$ is the parallel thermal velocity $(2T_\parallel^{\mathrm{ring}}/M)^{1/2}$ and $\Delta v_\perp$ the perpendicular thermal velocity implicitly determined by

$$\Delta v_\perp = (2T_\perp^{\mathrm{ring}}/M)^{1/2} \times \sqrt{\frac{\alpha_\perp}{\beta_\perp}} \quad (1c)$$

with

$$\beta_\perp = \exp\left(\frac{-V_{\mathrm{ring}}^2}{\Delta v_\perp^2}\right) + \sqrt{\frac{\pi}{2}}\frac{V_{\mathrm{ring}}}{\Delta v_\perp}\mathrm{erfc}\left(\frac{-V_{\mathrm{ring}}}{\Delta v_\perp}\right)$$

$$+ (d_\perp^4 - 1) + (d_\perp^3 - 1)\sqrt{\frac{\pi}{2}}\frac{V_{\mathrm{ring}}}{\Delta v_\perp}; \quad (1d)$$

Y is the step function, equal to 1 for positive values of its argument and 0 otherwise; $d_\perp$ is a given dilation coefficient that allows an increase ($d_\perp > 1$) or a decrease ($d_\perp < 1$) of the width of the ring distribution function for $v_\perp > V_{\mathrm{ring}}$, while for $v_\perp < V_{\mathrm{ring}}$ the distribution remains unchanged. Fig. 4 shows the distribution function plotted for $T_\perp^{\mathrm{ring}} = 0.4$ eV and $d_\perp = 1/2$ (curve a). It will be used with these parameters hereafter. For comparison, the ring distribution function used in the previous analysis is superimposed (curve b). The contribution of these protons to the dielectric tensor ($\bar{\bar{\epsilon}}_{\mathrm{ring}}$) has been determined by substituting (1) into the general expression of the dielectric tensor given by Ichimaru [1973, Eqs. (3.71)–(3.73), p. 51]. Its expression obtained after a substantial amount of algebraic calculations is reproduced in the Appendix. We have prescribed the contribution of the background torus plasma by the expression given by Ichimaru [1973, Eqs. (5.20)–(5.22), p. 89] which is valid for Maxwellian populations. The dispersion relation has been solved by computing these full expressions using the Mathematica software (Wolfram, 1991) that permits one to work with a precision exceeding 16 decimal digits. Naturally, this computation takes much more time than WHAMP computations but it allows us to characterize the unstable modes we are dealing with in a more realistic way, that is to say, with a more realistic distribution function of the pickup protons.

As a result, for $T_\parallel^{\mathrm{ring}} = 2$ eV, $T_\perp^{\mathrm{ring}} = 0.4$ eV and

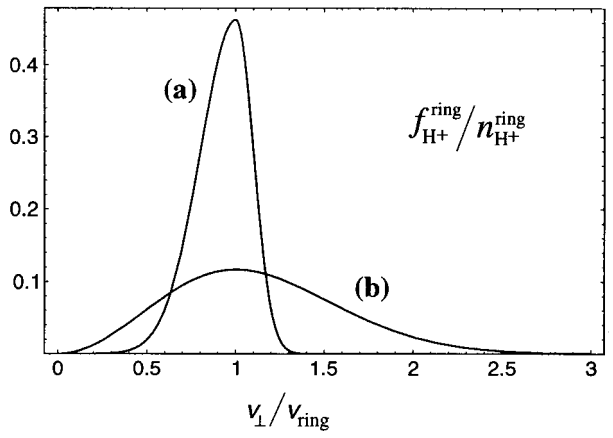

Fig. 4. Normalized ring distribution function we have used in the modified analysis (curve a). It is believed to be more realistic than the distribution function we have used in the WHAMP computations (curve b).

$d_\perp = 1/2$, (1) the ICW is stable whatever $\varepsilon_{H^+}^{ring}$ and (2) the IBCW is unstable for $\varepsilon_{H^+}^{ring} \geq 0.45\%$. The dispersion relation of IBCWs obtained by this computation for $\varepsilon_{H^+}^{ring} = 0.5\%$ is displayed in Fig. 6. Note that the proton ring distribution function we have used here is slightly less anisotropic than that used in the computations with WHAMP. This explains why ICWs are no longer destabilized in this last calculation. In fact, the ICW is sensitive to the anisotropy value as for a hydrodynamic mode. ICWs are indeed excited for small values of the wave number so that they propagate without finite Larmor radius effects ($k_\perp V_c \ll \Omega_{H^+}$). On the other hand, IBCW is sensitive to the shape of the ring distribution function as a resonant mode (e.g., it is stable for $d_\perp \geq 1$), and is not very sensitive to the anisotropy value. IBCWs are indeed excited for large values of $k_\perp$ so that they propagate with strong finite Larmor radius effects ($k_\perp V_c \geq \Omega_{H^+}$). As a matter of fact, in contrast to the growth rate γ obtained from WHAMP as a function of $k_\perp$ (Fig. 5, bottom panel), the growth rate profile obtained from our new algorithm is narrower (Fig. 6, bottom panel).

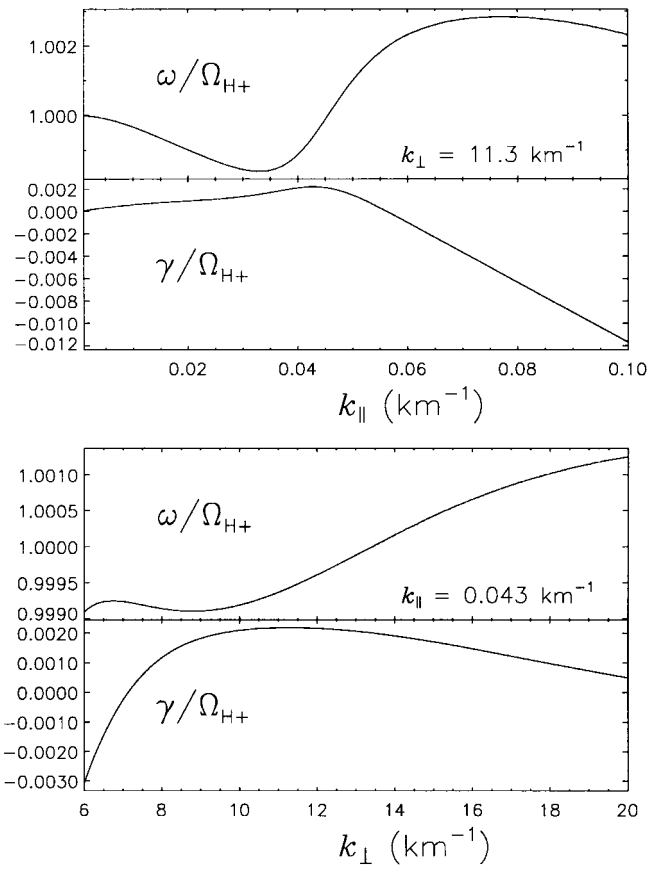

Fig. 5. Dispersion relation of the IBCWs computed for $\varepsilon_{H^+}^{ring} = 2.5\%$ with the WHAMP program (see the text). The top (bottom) panel shows the dispersion curve as a function of $k_\parallel$ ($k_\perp$), the value of $k_\perp$ ($k_\parallel$) being chosen to have the maximum growth rate.

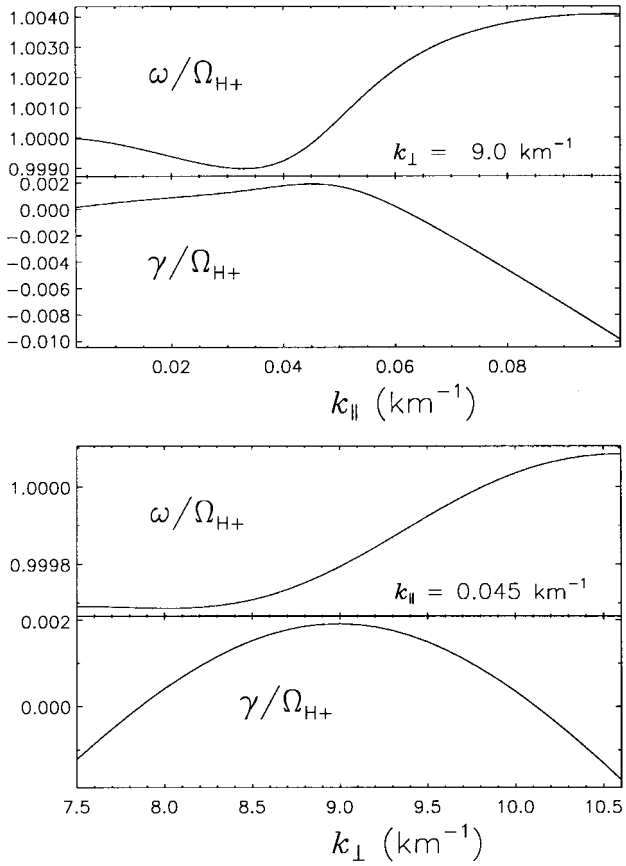

Fig. 6. Same as Fig. 5 but the dispersion relation is computed by using for the pickup protons the ring model given by (1), with $\varepsilon_{H^+}^{ring} = 0.5\%$, $T_\perp^{ring} = 0.4$ eV and $d_\perp = 1/2$.

4. Discussion

Assuming that the background torus plasma flowing around Io is mixed with ring protons, recently picked up from the Io's extended neutral cloud, two types of wave instability, IBCW and, eventually, ICW (if the anisotropy turned out to be very large), have been identified as possible candidates for explaining the observations presented above. In order to give more insight into the interpretation of these observations, the geometry of the encounter has now to be taken into account. In Fig. 2 of Kivelson et al. (1996a), for example, a view of the wake crossing by the Galileo spacecraft is presented. As evidenced in this figure, the near-Io trajectory is not exactly perpendicular to the wake axis so that the region crossed after the exit from the wake (inside Io's orbit) is located more downstream from Io than the region crossed before the entry into the wake (outside Io's orbit). This is probably the reason why there is a clear signature of spectral peaks inside Io's orbit while the signature is less clear outside Io's orbit (only seen occasionally on Fourier transformed wave form data). The waves have a perpendicular group velocity much smaller than the

corotation velocity ($V_g \ll V_c$) so that they are essentially moving with the corotating plasma. Given that these waves are generated by pickup protons near Io, roughly speaking in a sphere around Io, they convectively grow downstream from Io. Thus, the convective wave growth at a given point from Io will depend on the location with respect to the stream line. While approaching Io (beyond Io's orbit), Galileo was more upstream than while leaving Io (inside Io's orbit). Consequently, the integrated convective growth will be larger inside Io's orbit than outside Io's orbit. Indeed, insofar as the waves observed from about 17:50:00 to 17:54:00 UT are due to wave perturbations that have linearly grown, we can conclude that they have had enough time to convectively grow before their observation aboard the Galileo spacecraft. Then, let A be the corresponding amplification factor of these perturbations; one can reasonably assume that the convective growth should exceed 10 exponentiations,

$$A \geq e^{10} \tag{2}$$

to be extracted from noise. Being generated upstream at some typical distance L from Galileo's trajectory, they then grow during a time scale

$$t \sim \frac{L}{V_c} \tag{3}$$

before reaching Galileo. Inside Io's orbit, $L \sim 2R_{Io}$, while outside Io's orbit, L is roughly reduced by a factor 2. Assuming that the same wave instability takes place on both sides with the same growth rate γ, the corresponding amplification factors are given by $\exp(\gamma t)$. Thus, for the perturbations convectively growing outside Io's orbit, the amplification factor is only of the order of $\sqrt{A}$. Since $\sqrt{A} \gg 1$ and assuming that the amplitudes of the initial wave perturbations have the same order-of-magnitude on both sides, the amplitudes of the waves reaching Galileo outside Io's orbit have to be much smaller than the wave amplitudes observed inside Io's orbit, which explains the observed asymmetry.

The threshold value of γ used in the preceding section for determining the threshold value of $\varepsilon_{H^+}^{ring}$ for unstable waves can now be determined. Indeed, one gets from (2) and (3) that

$$\gamma \geq \frac{10 V_c}{L} \tag{4}$$

which leads, for $L \sim 2R_{Io}$, to a threshold value of about 0.16 s^{-1} for the growth rate. This corresponds to the value quoted above, namely, $\gamma/\Omega_{H^+} \geq 10^{-3}$.

As discussed above ICWs are little affected by Doppler-shift effects ($k_\perp V_c \ll \omega \approx \Omega_{H^+}$). Hence, the lack of observation at and below F_{H^+}, from about 17:50:00 to 17:54:00 UT, suggests that the waves observed during this period are not ICWs. Moreover, the ratio E/B for unstable ICWs would be about 5×10^5 m/s, which is one order-of-magnitude smaller than what is observed. Therefore, IBCWs remain the only viable candidate to explain the spectral peaks observed at about $2F_{H^+}$ and $4F_{H^+}$, as it will be shown hereafter.

First of all, the ratio E/B for unstable IBCWs are consistent with the observed values. In contrast to ICWs, IBCWs propagate for large values of $k_\perp$ so that Doppler-shift effects can be important. As a matter of fact, the dispersion relation shows that $k_\perp V_c \sim 3\Omega_{H^+}$ for the most unstable IBCWs excited at F_{H^+} (Fig. 6). The spacecraft velocity being, in the first approximation, negligible with respect to the corotation velocity, IBCWs excited in the downstream direction are thus observed at $\sim(1+3)F_{H^+}$, while IBCWs excited in the upstream direction are observed at $\sim(3-1)F_{H^+}$. This means that IBCWs are apparently not excited in a direction transverse to $\mathbf{V}_c$, since wave spectra do not present a continuum for frequencies between F_{H^+} and $4F_{H^+}$. Relatively narrow spectral peaks at about $2F_{H^+}$ and $4F_{H^+}$ are observed instead. As shown above, the use of a more realistic distribution function for pickup protons (in contrast to WHAMP's) gives a relatively narrow growth rate profile with respect to $k_\perp$. Doppler-shift can thus get a narrow range of frequencies.

The reason why IBCWs are mainly excited in the upstream and downstream directions can be understood as follows. The newly-created electron–proton pairs originating from the ionization of iogenic neutrals are injected into the background Jovian plasma with the velocity of Io, $-\mathbf{V}_c$. After several gyrations of the electrons but well before protons have time to rotate around $\mathbf{B}_0$, a current of protons is created that flows approximately towards the upstream direction. Due to the initial charge separation between the newborn protons and the newborn electrons, an electrostatic field approximately parallel to $\mathbf{V}_c$ has, therefore, to be created. On the other hand, in order to preserve charge neutrality, a current parallel to the background magnetic field is rapidly produced. The plane including both the background magnetic field and the flow line is, therefore, the plane in which the currents compensate. Faraday's law indicates that a magnetic field is then induced in a direction perpendicular to this plane. Naturally, the typical scale length of the spatial fluctuations associated with these electric and magnetic fields is about a fraction of the Larmor radius of the picked up protons (V_c/Ω_{H^+}). Start up conditions on the electric and magnetic fields select the eigenmodes that have both the wave vector and the wave polarization consistent with it. On this ground, one can conclude that the quasi-electrostatic IBCWs are predominantly excited along the flow lines in both the upstream and

downstream directions. Conversely, if one assumes that the spectral peaks, observed aboard the Galileo spacecraft are due to monochromatic waves (one wave frequency F) propagating in two opposite directions (Doppler-shifts $\pm\Delta F$), it has to be stressed that the frequencies observed for the spectral peaks, $\sim 2F_{H^+}$ and $\sim 4F_{H^+}$, determine in a unique way the wave frequency and the amplitude of the Doppler-shift as

$$F \sim F_{H^+} \quad \text{and} \quad \Delta F \sim 3F_{H^+} \tag{5}$$

respectively.

The free parameters in the calculation are those determining the ring shape ($T_{\parallel}^{\text{ring}}$, $T_{\perp}^{\text{ring}}$ and $d_{\perp}$) and the ring density ($\varepsilon_{H^+}^{\text{ring}}$). The other parameters, summarized in Table 1, are pulled out of the observations. The ring temperatures used, $T_{\parallel}^{\text{ring}} = 2$ eV and $T_{\perp}^{\text{ring}} = 0.4$ eV, can very likely be obtained from the rapid diffusion of the newly-picked up protons by transient electrostatic waves, pitch angle diffusion occurring faster than energy diffusion. For the dilation coefficient an intermediate value has been used, $d_{\perp} = 1/2$. Indeed, the most important thing is to have $d_{\perp} < 1$, in order to be consistent with the initial diffusion of the newly-picked up protons towards energies smaller than the injection energy (E_{ring}). We conclude that IBCWs excited by newly-picked up protons can explain in a rather simple way, the properties of the observed waves. The density of the newly-picked up proton must then be $\geq 0.5\%$ of the total density at about $2R_{\text{Io}}$ from Io's surface. The asymmetry of the observations with respect to the wake axis is explained by the fact that Galileo crossed Io's wake diagonally.

5. Io as an intrinsic source of protons?

From the data collected by the Galileo PWS experiment, the emissions observed in the low frequency range (5 to 200 Hz) during the close Io flyby on 7 December 1995 have been investigated. (1) Carrying out the dispersion analysis of the electromagnetic waves that can spontaneously develop in the plasma flowing near Io (first, by the use of WHAMP, then, by the use of a new algorithm that allows us to fit the distribution function of newborn ions in a more realistic way) and (2) taking into account the motion of the Galileo spacecraft relative to Io and the Jovian corotating plasma, it is possible to relate these observations to the existence of ring protons over a region of $> 2R_{\text{Io}}$ around Io. An extended neutral cloud of hydrogenic compounds around Io is thus inferred, at least in the equatorial region crossed by Galileo. The neutral cloud is partially broken up into its constituents and ionized by the ultraviolet light of the Sun and/or by impacts with the electrons and ions of the corotating plasma, thereby producing protons. Initially at rest with respect to Io, these newly-created protons are accelerated by the corotational electric field and begin to drift downstream with the Jovian magnetized plasma, forming a ring in velocity space. In particular, at about $2R_{\text{Io}}$ from Io's surface along the Galileo trajectory inside Io's orbit, the density of these freshly-picked up protons is found to be $\geq 0.5\%$ of the local plasma density (~ 4000 cm^{-3}), namely ≥ 20 cm^{-3}. By assuming that protons are created within $8R_{\text{Io}}$ of Io's surface, that the density of the pickup protons around Io's wake falls as r^{-n} with distance and that the pickup process is stationary, we can estimate a lower limit on the total amount of the newly-created protons which drift away from Io per unit time. For $n = 3$, we find that more than 3×10^{26} protons/s are created around Io.

Thus, Io acts as a source of protons in the Jovian magnetosphere. What is the origin of the inferred hydrogen? Hydrogen-bearing compounds other than H_2S might be present (Salama et al., 1994; Carlson et al., 1997). Do they ultimately originate from Io? Indeed, as suggested by the observation of caps of glowing hydrogen gas at the moon's poles (Roesler et al., 1999), the iogenic hydrogen might also result from the absorption of the Jovian magnetospheric proton current that flows into Io. In this case, Io would not really be a source of protons but a (more or less complex) relay station recycling Jovian magnetospheric protons.

Acknowledgements

We are grateful to G. Belmont for the many fruitful discussions. The French participation to this work is supported by CNRS and CNES.

Appendix A. Expression of $\overline{\overline{\varepsilon}}_{\text{ring}}$

The expression of the tensor $\overline{\overline{\varepsilon}}_{\text{ring}}$, as inferred from (1) and Ichimaru [1973, Eqs. (3.71)–(3.73), p. 51], normalized to the square of the ratio between the ring proton plasma frequency and the wave frequency, can be written as

$$\varepsilon_{yy}^{\text{ring}} = -1 + \frac{4\alpha_{\perp}^{-1}}{\Delta\beta_{\perp}^2} \sum_{n=-\infty}^{+\infty} \left[\frac{n}{\Delta\beta_{\parallel}} A_n(\beta_{\perp}, \Delta\beta_{\perp}) Z_0(z_n) + \frac{\Delta v_{\perp}^2}{\Delta v_{\parallel}^2} \frac{1}{\Delta\beta_{\perp}} B_n(\beta_{\perp}, \Delta\beta_{\perp}) Z_1(z_n) \right] \tag{A1a}$$

$$\varepsilon_{xx}^{\text{ring}} = -1 + \frac{4\alpha_\perp^{-1}}{\Delta\beta_\perp^2} \sum_{n=-\infty}^{+\infty} \left[\frac{n^3}{\Delta\beta_\parallel} C_n(\beta_\perp, \Delta\beta_\perp) Z_0(z_n) + \frac{\Delta v_\perp^2}{\Delta v_\parallel^2} \frac{n^2}{\Delta\beta_\perp} D_n(\beta_\perp, \Delta\beta_\perp) Z_1(z_n) \right] \quad \text{(A1b)}$$

$$\varepsilon_{xy}^{\text{ring}} = i\frac{4\alpha_\perp^{-1}}{\Delta\beta_\perp^2} \sum_{n=-\infty}^{+\infty} \left[\frac{n^2}{\Delta\beta_\parallel} E_n(\beta_\perp, \Delta\beta_\perp) Z_0(z_n) + \frac{\Delta v_\perp^2}{\Delta v_\parallel^2} \frac{n}{\Delta\beta_\perp} F_n(\beta_\perp, \Delta\beta_\perp) Z_1(z_n) \right] \quad \text{(A1c)}$$

$$\varepsilon_{xz}^{\text{ring}} = \frac{4\alpha_\perp^{-1}}{\Delta\beta_\perp \Delta\beta_\parallel} \sum_{n=-\infty}^{+\infty} \left[n^2 \frac{\Delta v_\parallel}{\Delta v_\perp} C_n(\beta_\perp, \Delta\beta_\perp) Z_1(z_n) + n\frac{k_\parallel}{k_\perp} D_n(\beta_\perp, \Delta\beta_\perp) Z_2(z_n) \right] \quad \text{(A1d)}$$

$$\varepsilon_{yz}^{\text{ring}} = -i\frac{4\alpha_\perp^{-1}}{\Delta\beta_\perp \Delta\beta_\parallel} \sum_{n=-\infty}^{+\infty} \left[n\frac{\Delta v_\parallel}{\Delta v_\perp} E_n(\beta_\perp, \Delta\beta_\perp) Z_1(z_n) + \frac{k_\parallel}{k_\perp} F_n(\beta_\perp, \Delta\beta_\perp) Z_2(z_n) \right] \quad \text{(A1e)}$$

$$\varepsilon_{zz}^{\text{ring}} = -1 + \frac{4}{\alpha_\perp} \sum_{n=-\infty}^{+\infty} \left[\frac{n}{\Delta\beta_\parallel} \frac{\Delta v_\parallel^2}{\Delta v_\perp^2} C_n(\beta_\perp, \Delta\beta_\perp) Z_2(z_n) + \frac{1}{\Delta\beta_\perp} D_n(\beta_\perp, \Delta\beta_\perp) Z_3(z_n) \right] \quad \text{(A1f)}$$

with

$$\varepsilon_{yx}^{\text{ring}} = -\varepsilon_{xy}^{\text{ring}}, \quad \varepsilon_{zx}^{\text{ring}} = +\varepsilon_{xz}^{\text{ring}}, \quad \varepsilon_{zy}^{\text{ring}} = -\varepsilon_{yz}^{\text{ring}} \quad \text{(A1g)}$$

where

$$z_n = \frac{\omega - n\Omega_{\text{H}^+}}{k_\parallel \Delta v_\parallel} \quad \text{(A1h)}$$

and

$$\beta_\perp = \frac{k_\perp V_{\text{ring}}}{\Omega_{\text{H}^+}}, \quad \Delta\beta_\perp = \frac{k_\perp \Delta v_\perp}{\Omega_{\text{H}^+}}, \quad \Delta\beta_\parallel = \frac{k_\parallel \Delta v_\parallel}{\Omega_{\text{H}^+}} \quad \text{(A1i)}$$

The functions A_n, B_n, C_n, D_n, E_n, and F_n determine the finite Larmor radius effects. They are defined by the following integrals:

$$A_n(\beta_\perp, \Delta\beta_\perp) = \int_{-\beta_\perp/\Delta\beta_\perp}^{+\infty} \mathrm{d}u \ \exp\left(\frac{-u^2}{d_u^2}\right) \times \frac{u}{d_u^2} (\beta_\perp + \Delta\beta_\perp u)^2 J_n'^2(\beta_\perp + \Delta\beta_\perp u) \quad \text{(A2a)}$$

$$B_n(\beta_\perp, \Delta\beta_\perp) = \int_{-\beta_\perp/\Delta\beta_\perp}^{+\infty} \mathrm{d}u \ \exp\left(\frac{-u^2}{d_u^2}\right) \times (\beta_\perp + \Delta\beta_\perp u)^3 J_n'^2(\beta_\perp + \Delta\beta_\perp u) \quad \text{(A2b)}$$

$$C_n(\beta_\perp, \Delta\beta_\perp) = \int_{-\beta_\perp/\Delta\beta_\perp}^{+\infty} \mathrm{d}u \ \exp\left(\frac{-u^2}{d_u^2}\right) \frac{u}{d_u^2} J_n^2(\beta_\perp + \Delta\beta_\perp u) \quad \text{(A2c)}$$

$$D_n(\beta_\perp, \Delta\beta_\perp) = \int_{-\beta_\perp/\Delta\beta_\perp}^{+\infty} \mathrm{d}u \ \exp\left(\frac{-u^2}{d_u^2}\right) (\beta_\perp + \Delta\beta_\perp u) J_n^2(\beta_\perp + \Delta\beta_\perp u) \quad \text{(A2d)}$$

$$E_n(\beta_\perp, \Delta\beta_\perp) = \int_{-\beta_\perp/\Delta\beta_\perp}^{+\infty} \mathrm{d}u \ \exp\left(\frac{-u^2}{d_u^2}\right) \frac{u}{d_u^2} \times (\beta_\perp + \Delta\beta_\perp u) J_n(\beta_\perp + \Delta\beta_\perp u) J_n'(\beta_\perp + \Delta\beta_\perp u) \quad \text{(A2e)}$$

$$F_n(\beta_\perp, \Delta\beta_\perp) = \int_{-\beta_\perp/\Delta\beta_\perp}^{+\infty} \mathrm{d}u \ \exp\left(\frac{-u^2}{d_u^2}\right) \times (\beta_\perp + \Delta\beta_\perp u)^2 J_n(\beta_\perp + \Delta\beta_\perp u) J_n'(\beta_\perp + \Delta\beta_\perp u) \quad \text{(A2f)}$$

d_u being the step function, equal to $d_\perp$ for positive values of u and 1 otherwise.

The velocity dispersion effects along the magnetic field are determined by the functions Z_j, $j = 0$ to 3, that are defined as

$$Z_j(\zeta) = \frac{1}{\sqrt{\pi}} \int_L \mathrm{d}t \frac{t^j \ \mathrm{e}^{-t^2}}{t - \zeta} \quad \text{(A3a)}$$

L being the Landau contour of integration that avoids the pole $t = \zeta$ by passing below. Thus, for $j = 0$, Z_j is merely the Fried and Conte's function (Fried and Conte, 1961) and, for $j = 1$ to 3, Z_j is related to this latter as follows:

$$Z_1(\zeta) = 1 + \zeta Z_0(\zeta) \quad \text{(A3b)}$$

$$Z_2(\zeta) = \zeta Z_1(\zeta) \tag{A3c}$$

$$Z_3(\zeta) = 1/2 + \zeta Z_2(\zeta) \tag{A3d}$$

References

Bagenal, F., 1994. Empirical model of the Io plasma torus: Voyager measurements. J. Geophys. Res. 99, 11043.

Carlson, R.W., Smythe, W.D., Lopes-Gautier, R.M.C., Davies, A.G., Kamp, L.W., Mosher, J.A., Soderblom, L.A., Leader, F.E., Mehlman, R., Clark, R.N., Fanale, F.P., 1997. The distribution of sulfur dioxide and other infrared absorbers on the surface of Io. Geophys. Res. Lett. 24, 2479.

Dendy, R.O., Lashmore-Davies, C.N., McClements, K.G., Cottrell, G.A., 1994. The excitation of obliquely propagating fast Alfvén waves at fusion ion cyclotron harmonics. Phys. Plasma 1, 1918.

Frank, L.A., Paterson, W.R., Ackerson, K.L., Vasyliunas, V.M., Coroniti, F.V., Bolton, S.J., 1996. Plasmas observations at Io with the Galileo spacecraft. Science 274, 394.

Fried, B.D., Conte, S.D., 1961. The Plasma Dispersion Function. Academic Press, New York.

Gurnett, D.A., Kurth, W.S., Shaw, R.R., Roux, A., Gendrin, R., Kennel, C.F., Scarf, F.L., Shawhan, S.D., 1992. The Galileo plasma wave investigation. Space Sci. Rev. 60, 341.

Gurnett, D.A., Kurth, W.S., Roux, A., Bolton, S.J., Kennel, C.F., 1996. The Galileo plasma wave observations in the Io plasma torus and near Io. Science 274, 391.

Hinson, D.P., Kliore, A.J., Flasar, F.M., Twicken, J.D., Schinder, P.J., Herrera, R.G., 1998. Galileo radio occultation measurements of Io's ionosphere and plasma wake. J. Geophys. Res. 103, 29,343.

Ichimaru, S., 1973. Basic Principles of Plasma Physics, A Statistical Approach. Benjamin-Cummings, Redwood City, CA.

Kivelson, M.G., Khurana, K.K., Means, J.D., Russell, C.T., Snare, R.C., 1992. The Galileo magnetic field investigation. Space Sci. Rev. 60, 357.

Kivelson, M.G., Khurana, K.K., Walker, R.J., Russell, C.T., Linker, J.A., Southwood, D.J., Polanskey, C., 1996a. A magnetic signature at Io: initial report from the Galileo magnetometer. Science 273, 337.

Kivelson, M.G., Khurana, K.K., Walker, R.J., Warnecke, J., Russell, C.T., Linker, J.A., Southwood, D.J., Polanskey, C., 1996b. Io's interaction with the plasma torus: Galileo magnetometer report. Science 274, 396.

Kliore, A.J., Fjeldbo, G., Seidel, B.L., Sweetnam, D.N., Sesplaukis, T.T., Woiceshyn, P.M., Rasool, S.I., 1975. The atmosphere of Io from Pioneer 10 radio occultation measurements. Icarus 24, 407.

Lellouch, E., Belton, M., de Pater, I., Paubert, G., Gulkis, S., Encrenaz, T., 1992. The structure, stability, and global distribution of Io's atmosphere. Icarus 98, 271.

Lellouch, E., 1996. Io's atmosphere: not yet understood. Icarus 124, 1.

Louarn, P., Perraut, S., Roux, A., Bolton, S., 1997. The global plasma environment of Io as inferred from the Galileo plasma wave observations. Geophys. Res. Lett. 24, 215.

McClements, K.G., Dendy, R.O., 1993. Ion cyclotron harmonic wave generation by ring protons in space plasmas. J. Geophys. Res. 98, 11,689.

McClements, K.G., Dendy, R.O., Lashmore-Davies, C.N., 1994. A model for the generation of obliquely propagating ULF waves near the magnetic equator. J. Geophys. Res. 99, 23,685.

Nash, D.B., Howell, R.R., 1989. Hydrogen sulfide: evidence from telescopic and laboratory infrared spectra. Science 244, 454.

Perraut, S., Roux, A., Robert, P., Gendrin, R., Sauvaud, J-A., Bosquet, J-M., Kremser, G., Korth, A., 1982. A systematic study of ULF waves above F_{H^+} from GEOS 1 and 2 measurements and their relationships with proton ring distributions. J. Geophys. Res. 87, 6219.

Roesler, F.L., Moos, H.W., Oliversen, R.J., Woodward Jr, R.C., Retherford, K.D., Scherb, F., McGrath, M.A., Smyth, W.H., Feldman, P.D., Strobel, D.F., 1999. Far-ultraviolet imaging spectroscopy of Io's atmosphere with HST/STIS. Science 283, 353.

Rönmark, K., 1982. WHAMP — waves in homogeneous, anisotropic multicomponent plasmas. Rep. 179. Kiruna Geophys. Inst., Kiruna, Sweden.

Salama, F., Allamandola, L.J., Witteborn, F.C., Cruikshank, D.P., Sandford, S.A., Bregman, J.D., 1990. The 2.5–5.0 μ spectra of Io: evidence for H_2S and H_2O frozen in SO_2. Icarus 83, 66.

Salama, F., Allamandola, L.J., Sandford, S.A., Bregman, J.D., Witteborn, F.C., Cruikshank, D.P., 1994. Is H_2O present on Io? The detection of a new strong band near 3590 cm^{-1} (2.79 μm). Icarus 107, 413.

Thomas, N., 1995. Ion temperatures in the Io plasma torus. J. Geophys. Res. 100, 7295.

Williams, D.J., Mauk, B.H., McEntire, R.E., Roelof, E.C., Amstrong, T.P., Wilken, B., Roederer, J.G., Krimigis, S.M., Fritz, T.A., Lanzerotti, L.J., 1996. Electron beams and ion composition measured at Io and in its torus. Science 274, 401.

Wolfram, S., 1991. Mathematica: A System for Doing Mathematics by Computers. Wolfram, Illinois.